Allosteric Tertiary Interactions Preorganize the c-di-GMP Riboswitch and Accelerate Ligand Binding

ARTICLE *in* ACS CHEMICAL BIOLOGY · MARCH 2012

Impact Factor: 5.33 · DOI: 10.1021/cb300014u · Source: PubMed

3 AUTHORS, INCLUDING:

David Rueda
Imperial College London
57 PUBLICATIONS **1,465** CITATIONS

SEE PROFILE

ACS chemical biology

Articles

pubs.acs.org/acschemicalbiology

Allosteric Tertiary Interactions Preorganize the c-di-GMP Riboswitch and Accelerate Ligand Binding

Sharla Wood,[†] Adrian R. Ferré-D'Amaré,*[,‡] and David Rueda*[,†]

[†]Department of Chemistry, Wayne State University, Detroit, Michigan, United States

[‡]National Heart, Lung and Blood Institute, Bethesda, Maryland, United States

Supporting Information

ABSTRACT: Cyclic diguanylate (c-di-GMP) is a bacterial second messenger important for physiologic adaptation and virulence. Class-I c-di-GMP riboswitches are phylogenetically widespread and thought to mediate pleiotropic genetic responses to the second messenger. Previous studies suggest that the RNA aptamer domain switches from an extended free state to a compact, c-di-GMP-bound conformation in which two helical stacks dock side-by-side. Single molecule fluorescence resonance energy transfer (smFRET) experiments now reveal that the free RNA exists in four distinct populations that differ in dynamics in the extended and docked conformations. In the presence of c-di-GMP and Mg^{2+}, a stably docked population (>30 min) becomes predominant. smFRET mutant analysis demonstrates that tertiary interactions distal to the c-di-GMP binding site strongly modulate the RNA population structure, even in the absence of c-di-GMP. These allosteric interactions accelerate ligand recognition by preorganizing the RNA, favoring rapid c-di-GMP binding.

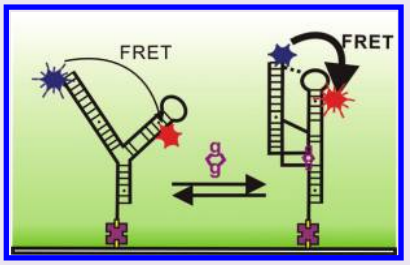

Riboswitches are gene-regulatory mRNA domains that recognize small molecule metabolites and second messengers.[1−8] With the exception of the catalytic *glmS* ribozyme-riboswitch,[9,10] these regulators function by adopting ligand occupancy-dependent conformations that modulate transcription, translation, or alternative splicing. The substructure of a riboswitch that suffices for specific ligand binding *in vitro* is known as its "aptamer" domain. Biophysical characterization of the aptamer domains of different riboswitch classes shows that their global structural response to ligand binding is idiosyncratic.[11] The aptamer domain of the flavin-mononucleotide (FMN) riboswitch from *Bacillus subtilis* is largely preorganized in the absence of FMN at physiologic Mg^{2+} concentrations, whereas that of the class I *S*-adenosylmethionine (SAM) riboswitch from the same organism is only partly ordered absent its cognate metabolite and adopts its most compact form upon SAM binding.[11] Moreover, the degree of compaction induced by ligand binding or by Mg^{2+} varies even between aptamer domains of the same riboswitch class [*e.g.*, the thiamine-pyrophosphate (TPP) riboswitches from *Escherichia coli* and *Arabidopsis thaliana*].[12] Although it has been suggested that this variation may reflect the distinct regulatory requirements of each genetic locus,[12] the functional significance of ligand binding-induced global folding of riboswitch aptamer domains remains to be established.

Cyclic diguanylate (c-di-GMP) is a bacterial second messenger involved in the regulation of a variety of complex physiological adaptations including motility, virulence, biofilm formation, and cell cycle progression.[13−16] Two structurally distinct classes of c-di-GMP riboswitches have been described.[17,18] Of these, the class I riboswitches (c-di-GMP-I) are the most widespread. Over 500 different c-di-GMP-I riboswitches have been identified in a wide range of bacteria and are often found in multiple copies in bacterial genomes. As many as 30 different genetic loci in *Geobacter uraniumreducens* appear to be under c-di-GMP-I riboswitch regulation.[19] Crystallographic structure determinations of the aptamer domain of the c-di-GMP-I riboswitch associated with the *tfoX* gene of *Vibrio cholerae* bound to the second messenger revealed that the RNA consists of three helices, paired regions P1a, P1b, and P2, joined in a three-way junction by joining regions J1a/b, J1b/2, and J2/1a (Figure 1a,b).[20,21] c-di-GMP binds at the junction, participating in an interaction network between P1a, P1b, and the three joining regions. The conserved A47 from J1b/2 intercalates between the two guanine bases of the second messenger (Figure 1a,b, purple). The bound c-di-GMP and A47 mediate continuous coaxial stacking between P1b and P1a. P2 docks side-by-side with P1b. This arrangement appears to be stabilized by two sets of phylogenetically conserved tertiary interactions distal to the junction, in addition to the c-di-GMP-bound junction itself. First, the GNRA tetraloop (GT) that caps P1b docks against a tetraloop receptor (TR) in P2. Second, an interhelical Watson−Crick pair is formed between C44 of P1b and G83 of P2 (Figure 1a,b, green and orange).[20,21]

Small-angle X-ray scattering (SAXS) experiments revealed a dramatic compaction of the class I riboswitch aptamer domain induced by c-di-GMP binding in the presence of physiologic [Mg^{2+}].[12,20] Low-resolution molecular envelopes calculated from the SAXS data suggest that, in absence of c-di-GMP, the RNA adopts an extended conformation in which P1b and P2

Received: January 11, 2012
Accepted: March 1, 2012
Published: March 1, 2012

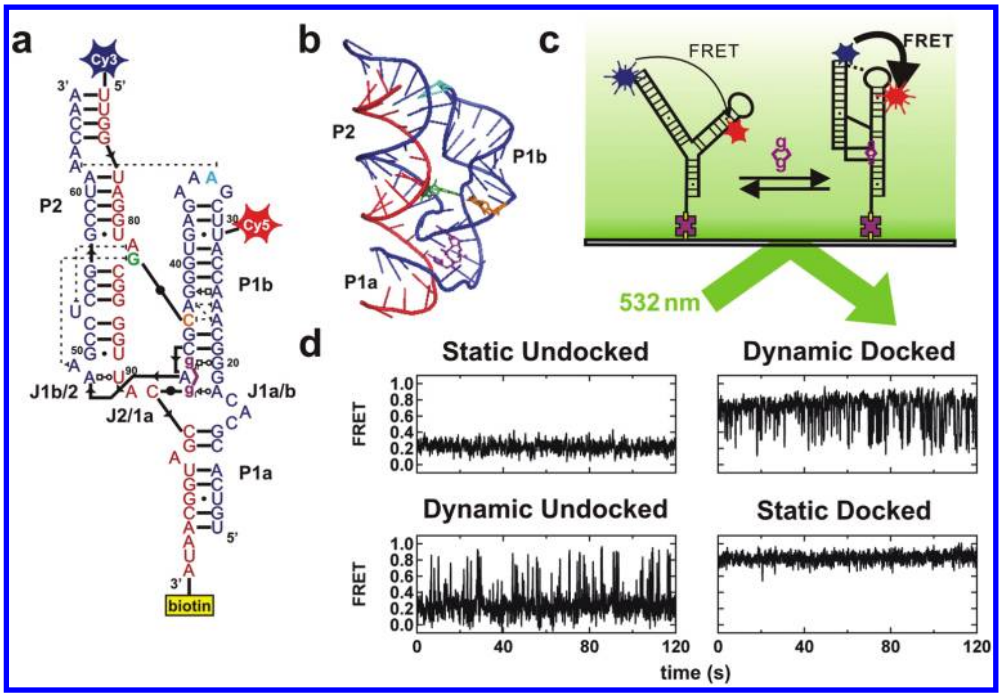

Figure 1. Single molecule FRET reveals four populations. (a) Secondary structure of the c-di-GMP-I riboswitch aptamer domain from *Vibrio cholerae* with c-di-GMP bound. For smFRET, a two-piece construct was used with the strands highlighted in red and blue. The red strand was covalently labeled with a Cy3 fluorophore on the 5′ end and a biotin on the 3′ end for immobilization to the quartz slide for smFRET experiments. The blue strand was internally labeled with a Cy5 fluorophore. Bound c-di-GMP is highlighted in purple, and G83C, C44A, and A33U mutations are highlighted in green, orange, and cyan, respectively. (b) Three-dimensional structure of the c-di-GMP-I riboswitch aptamer domain,[20] color-coded as in panel (a). (c) Schematic diagram of single molecule experiments. The RNA complex is immobilized to the quartz slide surface through a biotin-streptavidin bridge. The fluorophores are excited in a prism-based total internal reflection microscope. Fluorescence is collected through the objective and monitored with a CCD camera. (d) smFRET time trajectories. The static undocked population is identified by a static 0.2 FRET ratio. The dynamic docked population is identified by a mostly 0.8 FRET ratio with brief excursions to low FRET. The dynamic undocked population is identified by a mostly 0.2 FRET ratio with brief excursion to high FRET. The static docked population is identified by a static 0.8 FRET ratio.

are splayed apart, and neither the GT/TR interaction nor the C44·G83 base pairing takes place. Nuclease protection and in-line probing experiments are consistent with disruption of both sets of tertiary interactions in the absence of c-di-GMP, and also suggest that P1a becomes disordered under these conditions.[18,20] Previous studies of large catalytic RNAs have shown that tertiary interactions promote RNA folding within compact intermediates resulting from an early divalent cation-induced collapse, in which the helices interact but are not yet stably docked.[22] For instance, in the case of the *Azoarcus* group I ribozyme, a GT/TR interaction has been shown cooperatively to promote tertiary structure throughout the RNA, increasing the speed and accuracy of its folding.[23] Unlike these catalytic RNAs, which require only divalent cations to achieve their native state, riboswitch aptamer domains have evolved to recognize small molecules concomitant with folding.

To dissect the interplay of cations, second-messenger ligand and tertiary interactions in riboswitch folding, we have now analyzed the c-di-GMP-I aptamer domain using smFRET.[24−29] These studies confirm that this RNA samples extended and compact conformations. However, smFRET analysis, which can uncover structural dynamics of individual molecules that would otherwise be hidden in ensemble-averaged experiments, reveals that the aptamer domain is kinetically partitioned into four distinct populations: two that, in the experimental time frame, remain statically docked or undocked (compact or extended, respectively), one that fluctuates between docked and undocked but is preferentially in the docked state, and another that fluctuates but is preferentially undocked. The population structure shifts in response to Mg^{2+} and c-di-GMP concentration, such that at saturating second messenger and physiologic Mg^{2+} concentration, the majority of the molecules are statically docked. smFRET analysis of site-directed mutants that disrupt the GT/TR or C44·G83 tertiary interactions indicates that these not only are required for binding of c-di-GMP but also profoundly impact the population structure of the RNA in the absence of ligand. Thus, we find that these tertiary interactions, which are distant from the c-di-GMP binding site, serve to preorganize the aptamer domain. *In vivo*, this would allow the nascent riboswitch transcript to fold and recognize its ligand rapidly and thus respond effectively to varying intracellular levels of the second messenger.

RESULTS AND DISCUSSION

Single Molecule FRET Reveals Four Distinct Populations. We incorporated Cy3 (donor) and Cy5 (acceptor) fluorophores near the distal tips of P2 and P1b, respectively, of an RNA construct based on the *Vibrio cholerae tfoX* c-di-GMP riboswitch (Figure 1a−c).[29] With this labeling scheme, the extended conformation is expected to result in a low FRET ratio, while the compact conformation is expected to result in a high FRET ratio.[20] Characteristic smFRET time trajectories in standard conditions (which contain 2.5 mM Mg^{2+}, Methods) are shown in Figure 1d. The aptamer domain RNA exhibits FRET ratios of 0.2 and 0.8, which may correspond to the extended and docked conformations, respectively, deduced from the SAXS reconstructions.[20] States with intermediate FRET efficiencies were not observed with a time resolution of 33 ms

dx.doi.org/10.1021/cb300014u | *ACS Chem. Biol.* 2012, 7, 920−927

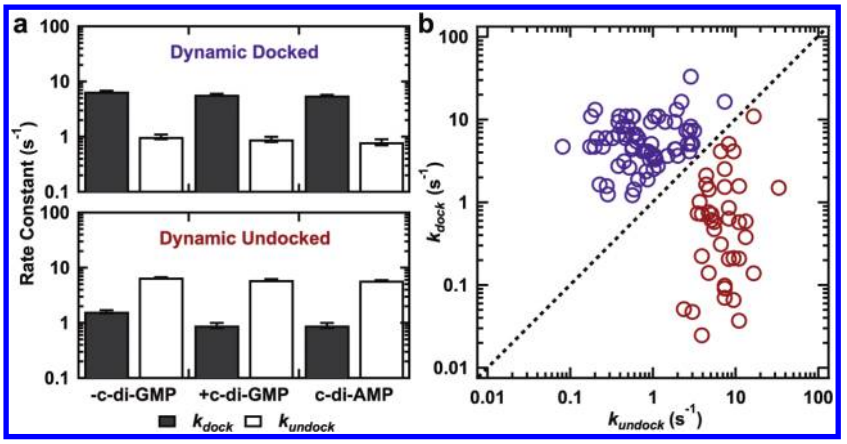

Figure 2. The dynamic populations do not have c-di-GMP bound. (a) Rate constants k_{dock} (black) and k_{undock} (white) for the dynamic docked and dynamic undocked populations in the absence of and presence of 100 nM c-di-GMP or presence of 1 μM c-di-AMP. The dwell time distributions were fit to single exponential decays to obtain k_{dock} and k_{undock}. (b) Scatter plot of the rate constants for both dynamic docked (purple) and dynamic undocked (red) populations in the absence of c-di-GMP demonstrates the existence of two distinct dynamic populations. The dynamic docked molecules lie above the diagonal, while the dynamic undocked lie below.

(Methods). In the absence of c-di-GMP, most molecules (49 ± 4% of 282, Supplemental Table 1) remain in a low FRET state over the time of the experiment (a few minutes). We refer to this population as static undocked. A smaller population (27 ± 5%) resides primarily in the high FRET state with brief excursions into the low FRET state. We refer to this population as dynamic docked. Two other minor populations are also observed: one in which molecules exhibit high FRET for the duration of the experiment (7 ± 2%), and another in which molecules display primarily low FRET with brief excursions into a high FRET state (17 ± 8%). We refer to these populations as static docked and dynamic undocked, respectively. We used dwell time analysis to determine the rate constants of docking and undocking for the two dynamic populations (Figure 2 and Supplemental Figure 1).[29] In the absence of c-di-GMP, k_{dock} and k_{undock} for the dynamic docked population are 6.6 ± 0.2 and 1.0 ± 0.1 s^{-1}, respectively, while k_{dock} and k_{undock} for the dynamic undocked population are 1.6 ± 0.1 and 6.7 ± 0.1 s^{-1}, respectively. Thus, the dynamic docked molecules spend most of the time in the docked conformation, and the dynamic undocked molecules spend most of the time in the undocked conformation. The distinct kinetic properties of these two populations become readily apparent by scatter analysis (Figure 2b).

In the presence of saturating c-di-GMP (1 μM, standard conditions, 2.5 mM Mg^{2+}, Methods), the static docked population becomes predominant (61 ± 4% of 250 molecules, Supplemental Table 1), suggesting that this population is ligand-bound. Both the static undocked and dynamic docked populations decrease significantly in the presence of ligand (to 29 ± 6% and 2 ± 2%, respectively). The docking and undocking rate constants for the dynamic populations in the presence of 100 nM c-di-GMP were similar to those in the absence of c-di-GMP (Figure 2 and Supplemental Figure 1), suggesting that these dynamic populations do not have c-di-GMP bound. Upon inspection of >100 time trajectories, we found that the static docked population can form from any of the other three populations (Figure 3a), providing further evidence that the static docked population is ligand-bound and indicating that any of these populations are able to bind c-di-GMP and form the stable docked conformation. Experiments with lower laser power and longer exposure showed the static

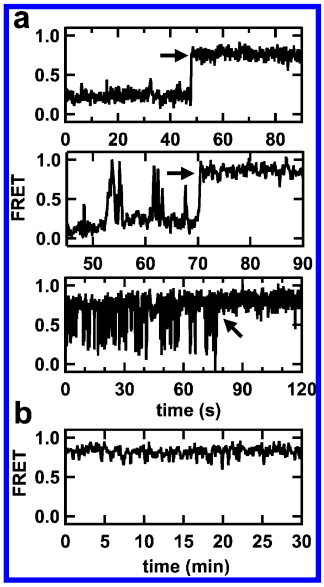

Figure 3. All aptamer domain populations can bind c-di-GMP. (a) smFRET time trajectories of the c-di-GMP-I riboswitch in the presence of 1 μM c-di-GMP showing formation of the static docked population from static undocked, dynamic undocked, and dynamic docked populations (top to bottom). Arrow indicates transition to the static docked population. (b) Single molecule FRET time trajectory showing the long-lived (at least 30 min) static docked population in the presence of 1 μM c-di-GMP.

docked conformation has a lifetime longer than 30 min (Figure 3b), consistent with previous results.[21]

To determine the second messenger binding affinity, we measured the fraction of c-di-GMP bound-riboswitch (static docked population) as a function of c-di-GMP concentration under standard conditions. In the absence of c-di-GMP, 7 ± 2% of riboswitches fold into the static docked conformation. This fraction increases with c-di-GMP concentration and saturates at 68 ± 9%, with the remaining molecules persisting in the undocked conformation. A fit to the Langmuir equation yields K_D = 90 ± 20 nM (Figure 4a,b), comparable with K_D's from isothermal titration calorimetry (ITC) experiments performed with single-chain aptamer domain constructs (Supplemental Table 2). This demonstrates the surface immobilization of the

dx.doi.org/10.1021/cb300014u | ACS Chem. Biol. 2012, 7, 920–927

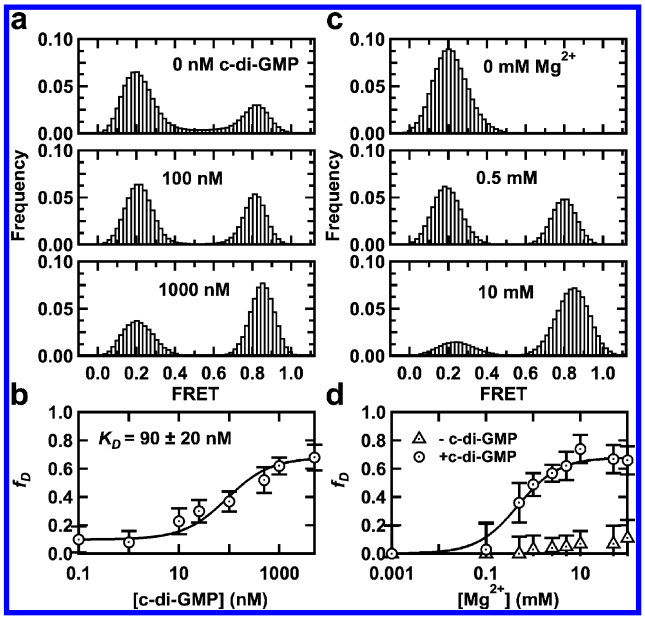

Figure 4. Formation of a stable docked conformation requires both c-di-GMP and Mg^{2+}. (a) smFRET histograms for >100 single molecule trajectories from all four populations combined as a function of the concentration of c-di-GMP, as indicated. In the absence of ligand, the low FRET (0.2) state predominates. As the concentration of c-di-GMP increases, the high FRET (0.8) state becomes more populated. (b) The fraction of static docked molecules (f_D) increases as a function of the conentration of c-di-GMP. The line is a fit to a modified Langmuir equation. Error bars are calculated based on the number of molecules. (c) smFRET histograms for >100 single molecule trajectories from all four populations combined in the presence of 1 μM c-di-GMP as a function of the concentration of Mg^{2+}, as indicated. At low Mg^{2+}, the low FRET state predominates. As the concentration of Mg^{2+} increases, the high FRET state becomes more populated. (d) The fraction of static docked molecules (f_D) increases as a function of the concentration of Mg^{2+} in the presence of 1 μM c-di-GMP (circles). The line is a fit to a modified Langmuir equation resulting in $K_{1/2}$ = 0.5 ± 0.1 mM. However, the fraction of static docked molecules (f_D) does not change significantly as a function of the concentration of Mg^{2+} in the absence of c-di-GMP (triangles). Error bars are calculated on the basis of the number of molecules.

two-chain RNA construct (Figure 1a) does not adversely affect folding or ligand binding. However, the affinity determined by smFRET and ITC is several orders of magnitude weaker than that based on electrophoretic gel mobility-shift analyses,[21] suggesting that the aptamer domain behaves differently in the polyacrylamide gel matrix.

To test the selectivity of the c-di-GMP-I riboswitch, we performed similar experiments using c-di-AMP, a structural analogue of c-di-GMP and recently discovered putative bacterial second messenger.[20,21,30] In bulk experiments, c-di-AMP does not bind the c-di-GMP-I riboswitch.[20,21] The aptamer domain displays similar behavior in smFRET experiments in the presence of 1 μM c-di-AMP as in the absence of c-di-GMP, with comparable population distributions (Supplemental Table 1). The docking and undocking rate constants for the dynamic molecules are also similar (Figure 2 and Supplemental Figure 1), supporting our interpretation that the dynamic molecules are not bound to the second messenger.

Overall, these data show the c-di-GMP-I riboswitch aptamer domain adopts docked and undocked conformations similar to those deduced from SAXS analysis.[20] The RNA is kinetically partitioned into four distinct populations that do not readily interconvert in the time frame of our experiments (several minutes) under steady-state conditions: static undocked and docked as well as dynamic undocked and docked. The RNA binds c-di-GMP tightly and selectively to fold into the stable docked conformation, and this results in population redistribution as the molecules in the three other populations are competent for second messenger binding.

Stable Docked Conformation Requires Both Mg^{2+} and c-di-GMP. Previous SAXS analysis of the *V. cholerae* c-di-GMP-I riboswitch aptamer domain indicates that the RNA undergoes global compaction as the concentration of Mg^{2+} is raised from 2.5 to 10 mM.[20] This is reminiscent of the behavior of other RNAs with complex structure, such as the group I intron and RNase P, which undergo Mg^{2+} ion-induced folding.[31−33] Those large ribozymes attain their native conformations upon Mg^{2+} ion-induced folding, as judged by their full catalytic activity.[34,35] In contrast, Kratky analysis of the SAXS data on the c-di-GMP-I aptamer domain implies that, unlike the group I intron and RNase P, the riboswitch remains locally disordered even at high Mg^{2+} concentration until c-di-GMP is bound.[20] Divalent cations can facilitate RNA folding nonspecifically, as part of a diffusely condensed ionic atmosphere, or by making specific, direct interactions with the RNA.[36] Our smFRET experiments indicate that both modes of action are operative in the c-di-GMP-I riboswitch.

To analyze the role of Mg^{2+} in c-di-GMP riboswitch folding, we measured the fraction of each RNA population as a function of [Mg^{2+}]. In the absence of both, Mg^{2+} and c-di-GMP, almost all of the molecules (96 ± 6% of 75 molecules) reside in the static undocked population (Supplemental Table 1). In the absence of Mg^{2+} ions, addition of saturating c-di-GMP does not alter the static undocked population. In very high [Mg^{2+}] (50 mM), but in the absence of c-di-GMP, the majority of molecules reside in the dynamic docked and undocked populations, as a consequence of a substantial decrease in the static undocked population. Fitting the fraction of dynamic molecules (including both dynamic docked and undocked) as a function of Mg^{2+} ion concentration to the Langmuir equation yields K_{Mg} = 1.2 ± 0.2 mM (Supplemental Figure 2). Even under these elevated [Mg^{2+}], only a small fraction of the molecules (10 ± 5%) are statically docked (Supplemental Table 1). These results indicate that both c-di-GMP and Mg^{2+} are necessary to drive a majority of the molecules into the static docked state and further support our assignment of this population to the ligand bound, highly structured conformation characterized crystallographically and by SAXS.[20]

To determine the interplay of Mg^{2+} ion and second messenger binding, we measured the fraction of c-di-GMP bound-riboswitch (static docked population) as a function of [Mg^{2+}]. In the presence of saturating c-di-GMP, the static docked population increases concomitant with increasing Mg^{2+} concentration (Figure 4c). Fitting the data to the Langmuir equation yields a K_{Mg} = 0.5 ± 0.1 mM (Figure 4d, circles), a value near the physiological range of concentration for the cation. In the absence of c-di-GMP, there is no increase in the static docked population (Figure 4d, triangles), indicating that Mg^{2+} and c-di-GMP binding are strongly cooperative. Experiments in the presence of higher monovalent ion concentrations but no Mg^{2+} (50 mM Tris-HCl, pH 8.0, 150 mM KCl, and 30 mM NaCl) show that the aptamer domain cannot fold into the docked conformation and remains entirely in the static undocked conformation even in the presence of saturating

dx.doi.org/10.1021/cb300014u | *ACS Chem. Biol.* 2012, 7, 920−927

c-di-GMP (Supplemental Table 1). These results suggest that the role of Mg^{2+} ions is not solely electrostatic screening required to fold the riboswitch into an ligand binding-competent conformation, but that it specifically mediates binding to the second messenger. Indeed, crystal structures reveal a hydrated Mg^{2+} ion at the second messenger-binding pocket[37] where it bridges a phosphate of c-di-GMP with those of residues G19 and G20 of the RNA, and our smFRET titration may be reporting on this tightly bound cation.

Tertiary Interactions Enable the Docked Conformation. To characterize the role of the GT/TR and C44·G83 tertiary interactions (Figure 1a)[20,21] in the formation and stability of the docked structure, we introduced point mutations to prevent their formation. First, we examined the C44·G83 base pair by mutating G83 to C. smFRET analyses of this G83C mutant show that both in the absence or presence of 1 μM c-di-GMP, most molecules (95 ± 9% and 80 ± 6%, respectively) reside in the static undocked population (Figure 5, Supplemental Table 1). The G83C mutant RNA is

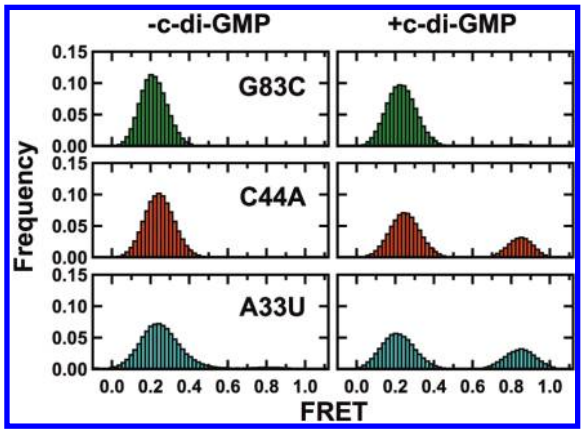

Figure 5. Tertiary interactions are necessary for the formation of the docked conformation. Single molecule FRET histograms are shown for >100 single molecule trajectories from riboswitch mutations with and without 1 μM c-di-GMP, as indicated. Colors correspond to the mutations shown in Figure 1a.

therefore unable to attain either the dynamic or static docked states, even with c-di-GMP present. These results are consistent with the results of bulk ITC experiments that show that the G83C mutant RNA is severely disrupted in c-di-GMP binding and exhibits a 1200-fold increase in the apparent K_D for c-di-GMP even at elevated Mg^{2+} concentration (10 mM) relative to wild-type RNA (Supplemental Table 2). Mutation of G83 to U also severely disrupts affinity for c-di-GMP with a 250-fold increase in K_D at 10 mM Mg^{2+} (Supplemental Table 2).

We also mutated C44 to A, which should prevent its interhelical base pairing with G83. smFRET experiments show that in the absence of c-di-GMP (Figure 5), the majority of the molecules (93 ± 3%) reside in the static undocked population. However, in the presence of 1 μM c-di-GMP this mutant exhibits a 25 ± 7% population in the static docked conformation (Figure 5, Supplemental Table 1), indicating that the C44A mutation does not destabilize the docked state as much as the G83C mutation. This result is also consistent with the binding affinity measured by bulk ITC, which shows an 80-fold increase in K_D at 10 mM Mg^{2+} (Supplemental Table 2) relative to wild-type. A possible explanation for this result is that the C44A mutant is capable of forming a non-canonical base pair with G83. Overall, these data show that the tertiary C44·G83 base pair is essential for the aptamer domain to attain either the dynamic or static docked states.

Next, we examined the role of the GT/TR interaction between P1b and P2 by mutating A33 to U (Figure 1a). The crystal structures show that A33 flips out of the GAAA tetraloop to stack with A62 of the TR.[20] Mutating A33 to U should prevent this stacking and therefore impair the GT/TR interaction. smFRET experiments using the A33U mutant in the absence of c-di-GMP show that the majority of molecules (68 ± 6%) reside in the static undocked population, but 29 ± 8% of the molecules reside in the dynamic undocked population (Supplemental Table 1). This result shows that, unlike mutations that affect the C44·G83 base pair, mutational destabilization of the GT/TR does not prevent the riboswitch from transiently populating the docked conformation. However, the addition of 20 mM Mg^{2+} was not able to recover the dynamic docked population. In the presence of 1 μM c-di-GMP, the fraction of the molecules in the static undocked population decreases to 49 ± 5% while the static docked population increases to 37 ± 3%, indicating that this mutant can still bind c-di-GMP and form the static docked conformation. This result is in agreement with gel shift experiments, which show a 200-fold increase in apparent K_D for this mutant.[37] These mutational data indicate that the C44·G83 base pair between P1b and P2 is essential for the formation of the stable docked conformation, while the GT/TR tertiary interaction assists in stabilizing the aptamer in the docked conformation. Overall, our smFRET analyses of riboswitch mutants indicate that docking of P1b and P2 mediated by long-range tertiary interactions is required for formation of a c-di-GMP binding-competent aptamer domain conformation.

Conclusions. Single molecule methods have previously been employed to examine several riboswitches. The adenine and guanine riboswitches are closely related RNAs organized around a three-helix junction, where the purine base binds. In the crystal structures of their ligand-bound aptamer domains,[38,39] the loops that close the distal ends of two of the constituent helices of the riboswitch associate through a series of tertiary interactions. smFRET and force spectroscopy experiments imply that some of these long-range interactions can take place in the presence of Mg^{2+} ions alone, prior to purine binding.[25,28,40−42] smFRET analyses of the class I and II SAM riboswitches suggest that these structurally unrelated RNAs can transiently sample conformations similar to their respective ligand-bound states in the presence solely of Mg^{2} and that SAM binding occurs by conformational capture.[26,27] The Mg^{2+}-induced, partially folded states of these riboswitches appear to be kinetic intermediates in pathways leading to their ligand-bound (native) states.[27,28,40] This supports the inference that the partially folded states of these RNAs have structural similarity to their native fold.

Like the purine and SAM riboswitches, the c-di-GMP riboswitch can transiently adopt a global fold similar to that of its second messenger-bound form in the presence of Mg^{2+} alone. However, the results of our smFRET analysis reveal that this RNA folds in a complex landscape, populated by four classes of molecules that interconvert very slowly in the time frame of the experiment. Such kinetic partitioning has been previously documented in bulk[43] and at the single-molecule level[44−47] for catalytic RNAs. The shift in the population structure of the RNA upon addition, first of physiologic concentrations of Mg^{2+} and then c-di-GMP, and the cooperativity

dx.doi.org/10.1021/cb300014u | ACS Chem. Biol. 2012, 7, 920−927

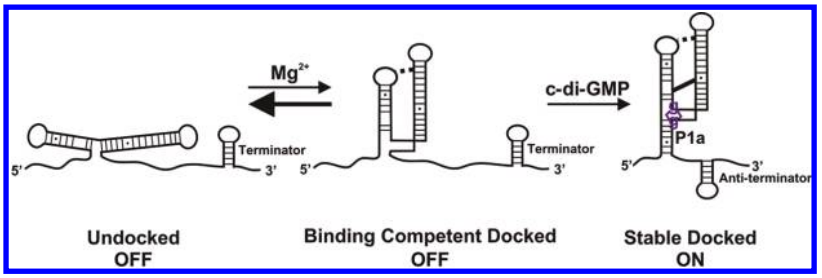

Figure 6. Proposed folding pathway of the c-di-GMP-I riboswitch. In the absence of c-di-GMP, the riboswitch adopts a stable undocked conformation, in which P1a is unpaired, allowing formation of the downstream terminator stem-loop and preventing gene expression. In the presence of Mg^{2+}, a population of dynamic riboswitches switch from a docked conformation with brief excursions into the undocked conformation. P1a, however, is not yet formed; therefore, the terminator stem-loop remains, preventing gene expression. This Mg^{2+}-dependent dynamic behavior offers a preorganized, ligand binding-competent structure that allows efficient cotranscriptional folding and c-di-GMP binding. Binding of c-di-GMP completes the formation of a continuous helical stack between P1a and P1b, which stabilizes the docked conformation, including the P1a helix; the anti-terminator stem forms, preventing formation of the terminator stem-loop, allowing transcription of the downstream gene to proceed.

exhibited by Mg^{2+} and c-di-GMP in formation of the stably docked population suggest that the high FRET state sampled by the dynamic undocked and dynamic docked populations has structural similarity to the native, second-messenger bound conformation. To provide support for this hypothesis, we generated RNAs with site-directed mutations targeting tertiary interactions that are present in the crystal structures of the ligand-bound aptamer domain. We first show calorimetrically that these mutant aptamer domains are impaired, to varying extents, in c-di-GMP binding. smFRET analysis reveals that the mutations perturb the folding landscape of the RNAs, such that decrease in the dynamic populations correlates directly with the deleterious impact of each mutation in ligand binding. This indicates that native-like tertiary interactions are indeed responsible for stabilizing the transiently folded states of the dynamic molecules, thereby demonstrating experimentally that the c-di-GMP riboswitch is preorganized, rather than simply collapsed. Since the dynamic populations shift to the static docked, ligand-bound conformation in the presence of c-di-GMP, the preorganization of the riboswitch enables rapid second messenger binding. Our findings parallel those of folding studies on large ribozymes, which have established the importance of forming native-like tertiary interactions early in the Mg^{2+}-induced collapse of an RNA in order to achieve overall rapid folding.[22]

The proposed folding pathway for the c-di-GMP riboswitch is shown in Figure 6. In the absence of c-di-GMP, the riboswitch adopts an undocked conformation. In-line and nuclease probing experiments indicate that, in the absence of ligand, P1a is unpaired, thus allowing the formation of the downstream terminator stem-loop and preventing gene expression.[18,20,21] A Mg^{2+}-dependent population of riboswitches exhibits dynamic switching from this undocked conformation to a docked conformation with brief excursions into the undocked conformation at transcription-relevant time scales (~150 ms). This unstable docked conformation is stabilized by the GT/TR and C44·G83 tertiary interactions. The co-crystal structures of the riboswitch[20,21] show that the nucleobase of A49 stacks underneath the C44·G83 base pair. This stacking may help propagate order from the interhelical base pair to the c-di-GMP binding site, in which A47 plays a central role (Figure 1a). The Mg^{2+}-dependent dynamic population offers a preorganized structure that allows efficient cotranscriptional folding and ligand binding. Upon binding to the junction region, c-di-GMP completes the formation of a continuous helical stack between P1a and P1b, leading to stabilization of the docked conformation, including the P1a helix. Although we did not directly determine formation of the P1a helix in our experiments, in-line and nuclease probing experiments and crystal structures indicate that this helix is formed in the folded aptamer domain structure.[18,20,21,37] This helix is the molecular switch controlling gene expression:[18] the anti-terminator stem would form, preventing formation of the terminator stem, allowing transcription of the downstream gene to proceed.

The biological significance of the large-scale, ligand-induced folding transition documented by SAXS for the c-di-GMP-I riboswitch has been unclear for two reasons. First, not every riboswitch class examined undergoes such a collapse concomitant with ligand binding.[11,12] Second, such large-scale reorganization of the aptamer domain couples the cost of the loss of conformational entropy to ligand recognition, thereby lowering the maximum achievable affinity. Our discovery that the c-di-GMP-I riboswitch aptamer domain transiently folds into a collapsed conformation that has a structure similar to that of the ligand-bound form suggests a role of the global folding transition in a process akin to kinetic proofreading: only molecules in which the P1b and P2 stems have folded correctly (*i.e.*, in conformations compatible with making the allosteric GT/TR and C44·G83 tertiary interactions) will present a ligand binding site to the second messenger. It is noteworthy that of the various riboswitches whose Mg^{2+}- and ligand-induced collapse has been studied by SAXS,[11,20,48,49] the TPP riboswitch is the RNA that most closely mimics the behavior of the c-di-GMP-I riboswitch. Although their specific sequences are unrelated, the aptamer domains of the c-di-GMP and TPP riboswitches share a similar architecture composed of a three-helix junction where the ligands bind and tertiary interactions distal to the ligand binding site stabilizing the side-by-side packing of two helical stems. Biophysical experiments have shown the importance of the allosteric loop−loop interactions in ligand binding by the TPP riboswitch.[50,51] These distal interactions were found to form before the TPP binding site is fully organized,[51] paralleling the results of our studies of the c-di-GMP-I riboswitch. Taken together, these studies suggest that large-scale preorganization coupled to ligand binding may be a strategy to increase structural specificity and hence accelerate ligand binding, by several riboswitch classes.

METHODS

RNA purification and labeling, single molecule FRET and Isothermal Titration Calorimetry experiments were performed as previously described.[11,20,29,52] A detailed description of the methods is available as Supporting Information online.

dx.doi.org/10.1021/cb300014u | *ACS Chem. Biol.* 2012, 7, 920−927

■ ASSOCIATED CONTENT

Supporting Information

This material is available free of charge *via* the Internet at http://pubs.acs.org.

■ AUTHOR INFORMATION

Corresponding Author

*E-mail: adrian.ferre@nih.gov; david.rueda@wayne.edu.

Notes

The authors declare no competing financial interest.

■ ACKNOWLEDGMENTS

We thank N. Kulshina for initial characterization of point mutants and N. Baird for calorimetry help. This work was supported in part by the National Institutes of Health (R01 GM085116) and an NSF CAREER award (MCB-0747285) to D.R. and in part by the intramural program of the National Heart, Lung and Blood Institute, NIH (A.R.F.)

■ REFERENCES

(1) Blouin, S., Mulhbacher, J., Penedo, J. C., and Lafontaine, D. A. (2009) Riboswitches: ancient and promising genetic regulators. *ChemBioChem 10*, 400−416.

(2) Edwards, T. E., Klein, D. J., and Ferré-D'Amaré, A. R. (2007) Riboswitches: small-molecule recognition by gene regulatory RNAs. *Curr. Opin. Struct. Biol. 17*, 273−279.

(3) Haller, A., Souliere, M. F., and Micura, R. (2011) The dynamic nature of RNA as key to understanding riboswitch mechanisms. *Acc. Chem. Res. 44*, 1339−1348.

(4) Montange, R. K., and Batey, R. T. (2008) Riboswitches: emerging themes in RNA structure and function. *Annu. Rev. Biophys. 37*, 117−133.

(5) Nahvi, A., Sudarsan, N., Ebert, M. S., Zou, X., Brown, K. L., and Breaker, R. R. (2002) Genetic control by a metabolite binding mRNA. *Chem. Biol. 9*, 1043.

(6) Roth, A., and Breaker, R. R. (2009) The structural and functional diversity of metabolite-binding riboswitches. *Annu. Rev. Biochem. 78*, 305−334.

(7) Smith, A. M., Fuchs, R. T., Grundy, F. J., and Henkin, T. M. (2010) Riboswitch RNAs: regulation of gene expression by direct monitoring of a physiological signal. *RNA Biol. 7*, 104−110.

(8) Zhang, J., Lau, M. W., and Ferré-D'Amaré, A. R. (2010) Ribozymes and riboswitches: modulation of RNA function by small molecules. *Biochemistry 49*, 9123−9131.

(9) Ferré-D'Amaré, A. R. (2010) The *glmS* ribozyme: use of a small molecule coenzyme by a gene-regulatory RNA. *Q. Rev. Biophys. 43*, 423−447.

(10) Winkler, W. C., Nahvi, A., Roth, A., Collins, J. A., and Breaker, R. R. (2004) Control of gene expression by a natural metabolite-responsive ribozyme. *Nature 428*, 281−286.

(11) Baird, N. J., and Ferré-D'Amaré, A. R. (2010) Idiosyncratically tuned switching behavior of riboswitch aptamer domains revealed by comparative small-angle X-ray scattering analysis. *RNA 16*, 598−609.

(12) Baird, N. J., Kulshina, N., and Ferré-D'Amaré, A. R. (2010) Riboswitch function: flipping the switch or tuning the dimmer? *RNA Biol. 7*, 328−332.

(13) Hengge, R. (2009) Principles of c-di-GMP signalling in bacteria. *Nat. Rev. Microbiol. 7*, 263−273.

(14) Jenal, U., and Malone, J. (2006) Mechanisms of cyclic-di-GMP signaling in bacteria. *Annu. Rev. Genet. 40*, 385−407.

(15) Schirmer, T., and Jenal, U. (2009) Structural and mechanistic determinants of c-di-GMP signalling. *Nat. Rev. Microbiol. 7*, 724−735.

(16) Tamayo, R., Pratt, J. T., and Camilli, A. (2007) Roles of cyclic diguanylate in the regulation of bacterial pathogenesis. *Annu. Rev. Microbiol. 61*, 131−148.

(17) Lee, E. R., Baker, J. L., Weinberg, Z., Sudarsan, N., and Breaker, R. R. (2010) An allosteric self-splicing ribozyme triggered by a bacterial second messenger. *Science 329*, 845−848.

(18) Sudarsan, N., Lee, E. R., Weinberg, Z., Moy, R. H., Kim, J. N., Link, K. H., and Breaker, R. R. (2008) Riboswitches in eubacteria sense the second messenger cyclic di-GMP. *Science 321*, 411−413.

(19) Weinberg, Z., Barrick, J. E., Yao, Z., Roth, A., Kim, J. N., Gore, J., Wang, J. X., Lee, E. R., Block, K. F., Sudarsan, N., Neph, S., Tompa, M., Ruzzo, W. L., and Breaker, R. R. (2007) Identification of 22 candidate structured RNAs in bacteria using the CMfinder comparative genomics pipeline. *Nucleic Acids Res. 35*, 4809−4819.

(20) Kulshina, N., Baird, N. J., and Ferré-D'Amaré, A. R. (2009) Recognition of the bacterial second messenger cyclic diguanylate by its cognate riboswitch. *Nat. Struct. Mol. Biol. 16*, 1212−1217.

(21) Smith, K. D., Lipchock, S. V., Ames, T. D., Wang, J., Breaker, R. R., and Strobel, S. A. (2009) Structural basis of ligand binding by a c-di-GMP riboswitch. *Nat. Struct. Mol. Biol. 16*, 1218−1223.

(22) Woodson, S. A. (2010) Compact intermediates in RNA folding. *Annu. Rev. Biophys. 39*, 61−77.

(23) Chauhan, S., and Woodson, S. A. (2008) Tertiary interactions determine the accuracy of RNA folding. *J. Am. Chem. Soc. 130*, 1296−1303.

(24) Aleman, E. A., Lamichhane, R., and Rueda, D. (2008) Exploring RNA folding one molecule at a time. *Curr. Opin. Chem. Biol. 12*, 647−654.

(25) Brenner, M. D., Scanlan, M. S., Nahas, M. K., Ha, T., and Silverman, S. K. (2010) Multivector fluorescence analysis of the xpt guanine riboswitch aptamer domain and the conformational role of guanine. *Biochemistry 49*, 1596−1605.

(26) Haller, A., Rieder, U., Aigner, M., Blanchard, S. C., and Micura, R. (2011) Conformational capture of the SAM-II riboswitch. *Nat. Chem. Biol. 7*, 393−400.

(27) Heppell, B., Blouin, S., Dussault, A. M., Mulhbacher, J., Ennifar, E., Penedo, J. C., and Lafontaine, D. A. (2011) Molecular insights into the ligand-controlled organization of the SAM-I riboswitch. *Nat. Chem. Biol. 7*, 384−392.

(28) Lemay, J. F., Penedo, J. C., Tremblay, R., Lilley, D. M., and Lafontaine, D. A. (2006) Folding of the adenine riboswitch. *Chem. Biol. 13*, 857−868.

(29) Zhao, R., and Rueda, D. (2009) RNA folding dynamics by single-molecule fluorescence resonance energy transfer. *Methods 49*, 112−117.

(30) Witte, G., Hartung, S., Buttner, K., and Hopfner, K. P. (2008) Structural biochemistry of a bacterial checkpoint protein reveals diadenylate cyclase activity regulated by DNA recombination intermediates. *Mol. Cell 30*, 167−178.

(31) Fang, X., Littrell, K., Yang, X. J., Henderson, S. J., Siefert, S., Thiyagarajan, P., Pan, T., and Sosnick, T. R. (2000) Mg^{2+}-dependent compaction and folding of yeast tRNAPhe and the catalytic domain of the B. subtilis RNase P RNA determined by small-angle X-ray scattering. *Biochemistry 39*, 11107−11113.

(32) Moghaddam, S., Caliskan, G., Chauhan, S., Hyeon, C., Briber, R. M., Thirumalai, D., and Woodson, S. A. (2009) Metal ion dependence of cooperative collapse transitions in RNA. *J. Mol. Biol. 393*, 753−764.

(33) Russell, R., Millett, I. S., Doniach, S., and Herschlag, D. (2000) Small angle X-ray scattering reveals a compact intermediate in RNA folding. *Nat. Struct. Biol. 7*, 367−370.

(34) Fang, X. W., Pan, T., and Sosnick, T. R. (1999) Mg^{2+}-dependent folding of a large ribozyme without kinetic traps. *Nat. Struct. Biol. 6*, 1091−1095.

(35) Rangan, P., Masquida, B., Westhof, E., and Woodson, S. A. (2003) Assembly of core helices and rapid tertiary folding of a small bacterial group I ribozyme. *Proc. Natl. Acad. Sci. U.S.A. 100*, 1574−1579.

(36) Draper, D. E. (2004) A guide to ions and RNA structure. *RNA 10*, 335−343.

(37) Smith, K. D., Lipchock, S. V., Livingston, A. L., Shanahan, C. A., and Strobel, S. A. (2010) Structural and biochemical determinants of

ligand binding by the c-di-GMP riboswitch. *Biochemistry 49*, 7351−7359.
(38) Batey, R. T., Gilbert, S. D., and Montange, R. K. (2004) Structure of a natural guanine-responsive riboswitch complexed with the metabolite hypoxanthine. *Nature 432*, 411−415.
(39) Serganov, A., Yuan, Y. R., Pikovskaya, O., Polonskaia, A., Malinina, L., Phan, A. T., Hobartner, C., Micura, R., Breaker, R. R., and Patel, D. J. (2004) Structural basis for discriminative regulation of gene expression by adenine- and guanine-sensing mRNAs. *Chem. Biol. 11*, 1729−1741.
(40) Greenleaf, W. J., Frieda, K. L., Foster, D. A., Woodside, M. T., and Block, S. M. (2008) Direct observation of hierarchical folding in single riboswitch aptamers. *Science 319*, 630−633.
(41) Neupane, K., Yu, H., Foster, D. A. N., Wang, F., and Woodside, M. T. (2011) Single-molecule force spectroscopy of the *add* adenine riboswitch relates folding to regulatory mechanism. *Nucleic Acids Res. 39*, 7677−7687.
(42) Tremblay, R., Lemay, J. F., Blouin, S., Mulhbacher, J., Bonneau, E., Legault, P., Dupont, P., Penedo, J. C., and Lafontaine, D. A. (2011) Constitutive regulatory activity of an evolutionarily excluded riboswitch variant. *J. Biol. Chem. 286*, 27406−27415.
(43) Pan, J., Thirumalai, D., and Woodson, S. A. (1997) Folding of RNA involves parallel pathways. *J. Mol. Biol. 273*, 7−13.
(44) Bokinsky, G., and Zhuang, X. (2005) Single-molecule RNA folding. *Acc. Chem. Res. 38*, 566−573.
(45) Ditzler, M. A., Rueda, D., Mo, J., Håkansson, K., and Walter, N. G. (2008) A rugged free energy landscape separates multiple functional RNA folds throughout denaturation. *Nucleic Acids Res. 36*, 7088−7099.
(46) Okumus, B., Wilson, T. J., Lilley, D. M. J., and Ha, T. (2004) Vesicle encapsulation studies reveal that single molecule ribozyme heterogeneities are intrinsic. *Biophys. J. 87*, 2798−2806.
(47) Zhuang, X., Bartley, L. E., Babcock, H. P., Russell, R., Ha, T., Herschlag, D., and Chu, S. (2000) A single-molecule study of RNA catalysis and folding. *Science 288*, 2048−2051.
(48) Ali, M., Lipfert, J., Seifert, S., Herschlag, D., and Doniach, S. (2010) The ligand-free state of the TPP riboswitch: a partially folded RNA structure. *J. Mol. Biol. 396*, 153−165.
(49) Lipfert, J., Das, R., Chu, V. B., Kudaravalli, M., Boyd, N., Herschlag, D., and Doniach, S. (2007) Structural transitions and thermodynamics of a glycine-dependent riboswitch from *Vibrio cholerae*. *J. Mol. Biol. 365*, 1393−1406.
(50) Kulshina, N., Edwards, T. E., and Ferré-D'Amaré, A. R. (2010) Thermodynamic analysis of ligand binding and ligand binding-induced tertiary structure formation by the thiamine pyrophosphate riboswitch. *RNA 16*, 186−196.
(51) Lang, K., Rieder, R., and Micura, R. (2007) Ligand-induced folding of the thiM TPP riboswitch investigated by a structure-based fluorescence spectroscopic approach. *Nucleic Acids Res. 35*, 5370−5378.
(52) Rueda, D., and Walter, N. G. (2006) Fluorescent energy transfer readout of an aptazyme-based biosensor. *Methods Mol. Biol. 335*, 289−310.